AIAA JOURNAL
Vol. 33, No. 10, October 1995

Postbuckling of Laminated Composites with Delaminations

Jaehong Lee,* Zafer Gürdal,† and O. Hayden Griffin Jr.‡
Virginia Polytechnic Institute and State University, Blacksburg, Virginia 24061-0219

Postbuckling analysis of laminated composites with delaminations is presented. A finite element method based on a layerwise laminated composite plate theory is developed to formulate and solve the problem. Geometric nonlinearity in the sense of von Kármán and imperfections in the form of initial global deflection and initial delamination openings are included. A simple contact algorithm which precludes the physically inadmissible overlapping between delaminated surfaces is proposed and incorporated into the analysis. Numerical results are obtained for through-the-width delaminations addressing the effects of the magnitude and direction of initial imperfections, laminate stacking sequence, and the contact condition between the delaminated surfaces on the postbuckling response. The proposed approach is shown to be efficient and powerful for solving the class of problems mentioned.

I. Introduction

DELAMINATION is a commonly observed damage mode in composite laminates and is known to cause degradation of overall stiffness and strength. In particular, delamination damage can result in substantial reduction in the buckling load of a laminate. In many cases, however, composite laminates are capable of carrying loads beyond their buckling loads and fail in the postbuckling regime. Furthermore, there may be a bending-extension coupling in debonded sublaminates, even if the undelaminated laminate is symmetric and free of initial imperfection, that will lead to geometrically nonlinear deformations. Therefore, in order to describe the damage process of delaminated composites up to final failure, bifurcation analysis may not be appropriate, and a postbuckling analysis may be required.

Several authors[1-5] have investigated various aspects of buckling and postbuckling behavior of delaminated structures using one-dimensional models. Effects of transverse shear deformation were studied by Kardomateas and Schmueser[6] and Kardomateas[7] by improving the model used in Ref. 1 for delamination buckling and growth in composite laminates. More recently, Chen[8] proposed a shear deformation theory using a variational energy principle. He found that the magnitude of the transverse shear effect depends on the delamination location and size.

Sheinman et al.[9] used a finite difference model to extend the work of Simitses et al.[2] to include the effect of bending-extension coupling on the stability of a delaminated composite. The effect of bending-extension coupling on postbuckling response was investigated by Yin[10] for both midplane delamination and thin-film delamination. Sheinman and Souffer[11] investigated the effects of bending-extension coupling and initial imperfection on the postbuckling behavior of a composite beam with various delamination geometries. It was found that the coupling effect significantly reduces the buckling load and increases the postbuckling deformations, and the global postbuckling deformation was shown to be very sensitive to initial imperfections. For some initial imperfections, however, the postbuckling analysis used in Ref. 11 exhibits physically inadmissible deformed shapes due to omission of the contact condition between delaminated sublaminates (i.e., the surfaces of the delamination are permitted to cross over each other).

Shear buckling and postbuckling behavior of a composite laminate with a delamination were investigated by Suemasu[12] by employing a no-penetration condition on the delaminated surfaces. The shear behavior of delaminated composites was found to be a combination of both local and global buckling modes. It was also reported that the postbuckling deformation exhibited sensitivity to initial imperfections.

The majority of the research cited employed either thin-film models or analytical models with four divided regions created by delamination in a composite laminate, see, for example, Ref. 1. In actual situations, however, such as when composite laminates are subjected to transverse impact loads, a number of delaminations with a very complicated configuration may occur. In an experimental study of compression response of axially loaded quasi-isotropic beams with multiple delaminations (delaminations introduced via three-point quasistatic bending load to simulate an impact condition), Breivik et al.[13] found that the beams containing short multiple through-the-width delaminations failed antisymmetrically at load levels lower than those containing long delaminations, which failed symmetrically. It is extremely difficult, if not impossible, to employ the existing analytical methods if there is more than one delamination with arbitrary boundary conditions. Therefore, there is a need for an analytical capability that can be applied to general multiple delaminations with complex geometry. Recently, Kutlu and Chang[14] proposed an analytical model to simulate the compression response of laminated composites containing multiple delaminations. They found that multiple delaminations can reduce the load-carrying capacity more than a single delamination.

The buckling loads and corresponding mode shapes of a laminated composite containing multiple delaminations were recently studied using a layerwise approach by Lee et al.[15] based on Reddy's layer-wise theory.[16] It was found that the antisymmetric buckling mode is dominant for a composite laminate having short multiple delaminations as experimentally shown by Breivik et al.[13] It was also shown that the buckling mode shapes for a midplane delaminated composite depend on the slenderness of the laminate.

In the present study, the analytical approach of Ref. 15 is extended to provide an appropriate analysis for the postbuckling behavior of a delaminated composite laminate with initial imperfections. The approach addresses the geometrically nonlinear deformation of the beam and the delaminated surfaces and their instability as a function of the applied compressive loads. However, the fracture mechanics problem associated with delamination growth due to crack opening displacements are ignored in the present study. Numerical results are presented for postbuckling problems of composites with through-the-width delaminations. Both single and multiple delamination problems are studied in the framework of geometric nonlinear postbuckling analysis. The effects of initial imperfections, contact condition between delaminated surfaces, and laminate stacking sequences are investigated.

Received April 28, 1993; revision received March 15, 1995; accepted for publication March 15, 1995.

*Postdoctoral Research Associate, Department of Engineering Science and Mechanics; currently at Hyundai Institute of Construction Technology, Republic of Korea. Member AIAA.

†Professor, Department of Engineering Science and Mechanics. Associate Fellow AIAA.

‡Professor, Department of Engineering Science and Mechanics. Senior Member AIAA.

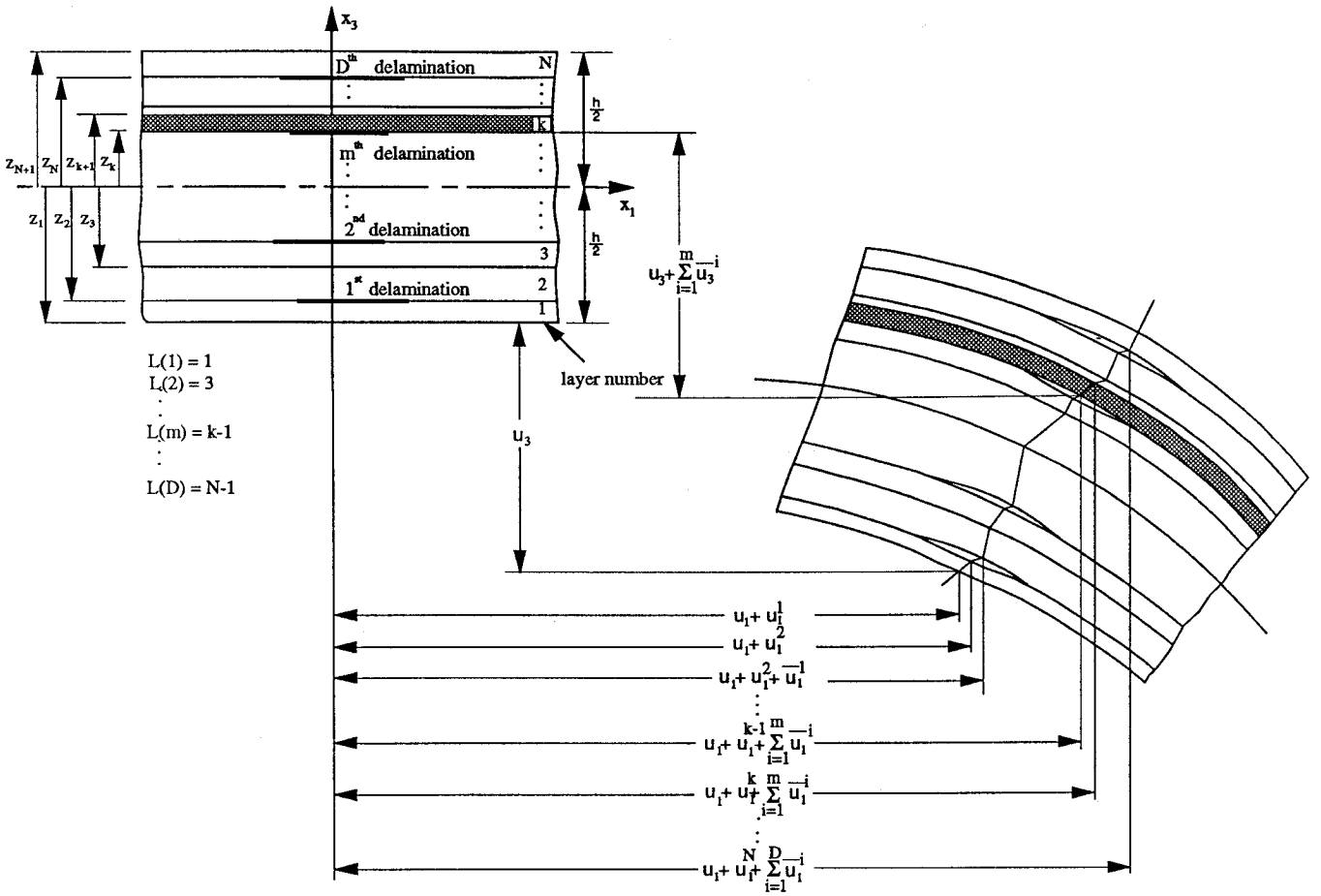

Fig. 1 Configuration of kinematics of a laminated composite with delaminations.

II. Theoretical Formulation

A. Kinematics

An N-layer fiber-reinforced composite beam-plate containing multiple through-the-width delaminations is considered. To model the multiple delaminations, the assumed displacement field is supplemented with unit step functions which allow discontinuities in the displacement field. The resulting displacements U_α and U_3 at a generic point x_1, x_2, x_3 in the laminate are assumed to be of the form

$$U_\alpha(x_\beta, x_3) = u_\alpha(x_\beta) + \phi^j(x_3)u^j_\alpha(x_\beta) + \delta^i(x_3)\bar{u}^i_\alpha(x_\beta) \tag{1}$$

$$U_3(x_\beta, x_3) = u_3(x_\beta) + \delta^i(x_3)\bar{u}^i_3(x_\beta) \tag{2}$$

The usual Cartesian indicial notation is employed where Greek subscripts are assumed to have values 1–2. Superscripts i and j range from 1 to D and from 1 to N, respectively, where D is the number of delaminations and N is the number of layers. The terms u_α and u_3 are the displacements of a point $(x_\beta, 0)$ on the reference surface of the laminate, u^j_α are nodal values of the displacements in the x_α direction of each equivalent single layer, and $\bar{u}^i_\alpha$ and $\bar{u}^i_3$ represent possible jumps in the slipping and opening displacements, respectively, at the $L(i)$th delaminated interface. $L(i)$th denotes the location of the interface where the ith delamination lies (see Fig. 1). The term $\phi^j(z)$ is the linear through-the-thickness Lagrangian interpolation function of the laminate, and $\delta^i(z)$ is the unit step function.

Following the procedure in Chia,[17] the nonlinear strain tensor with initial plate curvature in the sense of von Kármán nonlinearity is derived. Neglecting the quadratic terms in the in-plane displacements u_α, u^j_α, and $\bar{u}^i_\alpha$, the nonlinear strain tensor is given by

$$ds^2 - ds_0^2 = 2(\epsilon_{\alpha\beta}\,dx_\alpha\,dx_\beta + \gamma_{\alpha 3}\,dx_\alpha\,dx_3) \tag{3}$$

where $\epsilon_{\alpha\beta}$ and $\gamma_{\alpha 3}$ are the nonlinear strain tensors given by

$$\begin{aligned}\epsilon_{\alpha\beta} &= \epsilon^0_{\alpha\beta} + \phi^j\epsilon^j_{\alpha\beta} + \delta^i\bar{\epsilon}^i_{\alpha\beta} + \delta^i\delta^s\bar{\epsilon}^{is}_{\alpha\beta}\\ \gamma_{\alpha 3} &= \gamma^0_{\alpha 3} + \phi^j_3\gamma^j_{\alpha 3} + \delta^i\bar{\gamma}^i_{\alpha 3}\end{aligned} \tag{4}$$

and

$$\epsilon^0_{\alpha\beta} = \tfrac{1}{2}\left[u_{\alpha,\beta} + u_{\beta,\alpha} + \tfrac{1}{2}u_{3,\alpha}(u_3 + 2\xi)_{,\beta} + \tfrac{1}{2}u_{3,\beta}(u_3 + 2\xi)_{,\alpha}\right] \tag{5}$$

$$\epsilon^j_{\alpha\beta} = \tfrac{1}{2}\left(u^j_{\alpha,\beta} + u^j_{\beta,\alpha}\right) \tag{6}$$

$$\begin{aligned}\bar{\epsilon}^i_{\alpha\beta} = \tfrac{1}{2}\Big[&\bar{u}^i_{\alpha,\beta} + \bar{u}^i_{\beta,\alpha} + \tfrac{1}{2}u_{3,\alpha}\left(\bar{u}^i_3 + 2\bar{\xi}^i\right)_{,\beta} + \tfrac{1}{2}u_{3,\beta}\left(\bar{u}^i_3 + 2\bar{\xi}^i\right)_{,\alpha}\\ &+ \tfrac{1}{2}\bar{u}^i_{3,\alpha}(u_3 + 2\xi)_{,\beta} + \tfrac{1}{2}\bar{u}^i_{3,\beta}(u_3 + 2\xi)_{,\alpha}\Big]\end{aligned} \tag{7}$$

$$\bar{\epsilon}^{is}_{\alpha\beta} = \tfrac{1}{4}\left[\bar{u}^i_{3,\alpha}\left(\bar{u}^s_3 + 2\bar{\xi}^s\right)_{,\beta} + \bar{u}^s_{3,\beta}\left(\bar{u}^i_3 + 2\bar{\xi}^i\right)_{,\alpha}\right] \tag{8}$$

$$\gamma^0_{\alpha 3} = u_{3,\alpha}, \qquad \gamma^j_{\alpha 3} = u^j_\alpha, \qquad \bar{\gamma}^i_{\alpha 3} = \bar{u}^i_{3,\alpha} \tag{9}$$

In the preceding expressions, ξ and $\bar{\xi}^i$ are defined as the global imperfection shape of the plate and the shape of an initial opening of each delamination, respectively.

B. Variational Formulation

The principle of virtual displacements is used to derive the governing equilibrium equation of the present theory,

$$0 = \int_V (\sigma_{\alpha\beta}\delta\epsilon_{\alpha\beta} + \sigma_{\alpha 3}\delta\gamma_{\alpha 3} - f_i\delta U_i)\,dV - \oint_S \hat{t}_i\delta U_i\,dS \tag{10}$$

where $\hat{t}_i$ are the specified surface traction forces and f_i are the body forces ($i = 1, 2, 3$). In Eq. (10), V is the volume of the plate and

S is the portion of the boundary of V on which the tractions are specified.

Substituting Eq. (4) into Eq. (10) and integrating through the thickness, in the absence of body forces, Eq. (10) takes the following form:

$$
\begin{aligned}
0 = \int_\Omega & \left[N_{\alpha\beta}\{\delta u_{\alpha,\beta} + \delta u_{3,\alpha}(u_3+\xi)_{,\beta}\} + N^j_{\alpha\beta}\delta u^j_{\alpha,\beta}\right. \\
& + \bar{N}^i_{\alpha\beta}\left\{\delta\bar{u}^i_{\alpha,\beta} + \delta u_{3,\alpha}\left(\bar{u}^i_3+\bar{\xi}^i\right)_{,\beta} + \delta\bar{u}^i_{3,\alpha}(u_3+\xi)_{,\beta}\right\} \\
& + \tfrac{1}{2}\bar{N}^{is}_{\alpha\beta}\left\{\delta\bar{u}^i_{3,\alpha}\left(\bar{u}^s_3+\bar{\xi}^s\right)_{,\beta} + \delta\bar{u}^s_{3,\beta}\left(\bar{u}^i_3+\bar{\xi}^i\right)_{,\alpha}\right\} \\
& \left. + Q_{\alpha 3}\delta u_{3,\alpha} + Q^j_{\alpha 3}\delta u^j_\alpha + \bar{Q}^i_{\alpha 3}\delta\bar{u}^i_{3,\alpha}\right]\mathrm{d}x_1\mathrm{d}x_2 \\
& - \int_\Omega p\delta\left(u_3 + \delta^i\bar{u}^i_3\right)\mathrm{d}x_1\mathrm{d}x_2 \\
& - \int_{\Gamma_1}\hat{N}_\alpha\delta u_\alpha\,\mathrm{d}S - \int_{\Gamma_2}\hat{Q}_3\delta u_3\,\mathrm{d}S - \int_{\Gamma_3}\hat{N}^j_\alpha\delta u^j_\alpha\,\mathrm{d}S \\
& - \int_{\Gamma_4}\hat{\bar{N}}^i_\alpha\delta\bar{u}^i_\alpha\,\mathrm{d}S - \int_{\Gamma_5}\hat{\bar{Q}}^i_3\delta u^i_3\,\mathrm{d}S
\end{aligned}
\tag{11}
$$

where p is a specified distributed transverse load and Γ_1, Γ_2, Γ_3, Γ_4, and Γ_5 are the portions of the boundary of the reference surface Ω on which $\hat{N}_\alpha$, $\hat{Q}_3$, $\hat{N}^j_\alpha$, $\hat{\bar{N}}^i_\alpha$, $\hat{\bar{Q}}^i_3$, respectively, are specified. In Eq. (11), the stress resultants are defined as

$$
\begin{aligned}
\left[N_{\alpha\beta}, N^j_{\alpha\beta}, \bar{N}^i_{\alpha\beta}, \bar{N}^{is}_{\alpha\beta}\right] &= \int_{z_k}^{z_{k+1}}\sigma_{\alpha\beta}[1, \phi^j, \delta^i, \delta^i\delta^s]\,\mathrm{d}x_3 \\
\left[Q_{\alpha 3}, Q^j_{\alpha 3}, \bar{Q}^i_{\alpha 3}\right] &= \int_{z_k}^{z_{k+1}}\sigma_{\alpha 3}\left[1, \phi^j_3, \delta^i\right]\mathrm{d}x_3
\end{aligned}
\tag{12}
$$

and the specified traction resultants are defined as

$$
\begin{aligned}
\left(\hat{N}_\alpha, \hat{N}^j_\alpha, \hat{\bar{N}}^i_\alpha\right) &= \int_{z_k}^{z_{k+1}}\hat{t}_\alpha(1, \phi^j, \delta^i)\,\mathrm{d}x_3 \\
\left(\hat{Q}_3, \hat{\bar{Q}}^i_3\right) &= \int_{z_k}^{z_{k+1}}\hat{t}_3(1, \delta^i)\,\mathrm{d}x_3
\end{aligned}
\tag{13}
$$

C. Equilibrium Equations

The equilibrium equations of the present theory can be derived by integrating the derivatives of the varied quantities by parts and collecting the coefficients of δu_α, δu_3, δu^j_α, $\delta\bar{u}^i_\alpha$, and $\delta\bar{u}^i_3$:

$$N_{\alpha\beta,\alpha} = 0 \tag{14}$$

$$Q_{\beta 3,\beta} + [N_{\alpha\beta}(u_{3,\alpha}+\xi_{,\alpha})]_{,\beta} + \left[\bar{N}^i_{\alpha\beta}\left(\bar{u}^i_{3,\alpha}+\bar{\xi}^i_{,\alpha}\right)\right]_{,\beta} = 0 \tag{15}$$

$$N^j_{\alpha\beta,\alpha} - Q^j_{\beta 3} = 0 \tag{16}$$

$$\bar{N}^i_{\alpha\beta,\alpha} = 0 \tag{17}$$

$$\bar{Q}^i_{\beta 3,\beta} + \left[\bar{N}^i_{\alpha\beta}(u_{3,\alpha}+\xi_{,\alpha})\right]_{,\beta} + \left[\bar{N}^{is}_{\alpha\beta}\left(\bar{u}^s_{3,\alpha}+\bar{\xi}^s_{,\alpha}\right)\right]_{,\beta} = 0 \tag{18}$$

These equilibrium equations consist of $(3+2N+3D)$ differential equations in $(3+2N+3D)$ variables $(u_\alpha, u_3, u^j_\alpha, \bar{u}^i_\alpha, \bar{u}^i_3)$. The geometric nonlinearity is present only in Eqs. (15) and (18), which represent the out-of-plane equilibrium of the laminate and the sublaminates.

The boundary conditions are of the form

$$
\begin{aligned}
&\delta u_\alpha\text{:} && N_\alpha - \hat{N}_\alpha = 0 && \text{or} && u_\alpha = \hat{u}_\alpha \\
&\delta u_3\text{:} && Q_3 - \hat{Q}_3 = 0 && \text{or} && u_3 = \hat{u}_3 \\
&\delta u^j_\alpha\text{:} && N^j_\alpha - \hat{N}^j_\alpha = 0 && \text{or} && u^j_\alpha = \hat{u}^j_\alpha \\
&\delta\bar{u}^i_\alpha\text{:} && \bar{N}^i_\alpha - \hat{\bar{N}}^i_\alpha = 0 && \text{or} && \bar{u}^i_\alpha = \hat{\bar{u}}^i_\alpha \\
&\delta\bar{u}^i_3\text{:} && \bar{Q}^i_3 - \hat{\bar{Q}}^i_3 = 0 && \text{or} && \bar{u}^i_3 = \hat{\bar{u}}^i_3
\end{aligned}
\tag{19}
$$

where

$$
\begin{aligned}
N_\alpha &= N_{\alpha\beta}n_\beta \\
Q_3 &= \left[N_{\alpha\beta}(u_3+\xi)_{,\alpha} + \bar{N}^i_{\alpha\beta}\left(\bar{u}^i_3+\bar{\xi}^i\right)_{,\alpha} + Q_{\beta 3}\right]n_\beta \\
N^j_\alpha &= N^j_{\alpha\beta}n_\beta \\
\bar{N}^i_\alpha &= \bar{N}^i_{\alpha\beta}n_\beta \\
\bar{Q}^i_3 &= \left[\bar{N}^i_{\alpha\beta}(u_3+\xi)_{,\alpha} + \bar{N}^{is}_{\alpha\beta}\left(\bar{u}^s_3+\bar{\xi}^s\right)_{,\alpha} + \bar{Q}^i_{\beta 3}\right]n_\beta
\end{aligned}
\tag{20}
$$

D. Constitutive Equations

The constitutive equations of the kth orthotropic lamina in the laminate coordinate system are given by

$$
\begin{aligned}
\sigma^{(k)}_{\alpha\beta} &= \bar{Q}^{(k)}_{\alpha\beta\gamma\omega}\epsilon^{(k)}_{\gamma\omega} \\
\sigma^{(k)}_{\alpha 3} &= \bar{Q}^{(k)}_{\alpha 3\beta 3}\gamma^{(k)}_{\beta 3}
\end{aligned}
\tag{21}
$$

where $[\bar{Q}]^{(k)}$ denotes the transformed reduced stiffness matrix of the kth layer.

Substitution of Eq. (21) into Eq. (13) gives the constitutive equations of the laminate,

$$
\begin{Bmatrix} N_{\alpha\beta} \\ N^j_{\alpha\beta} \\ \bar{N}^i_{\alpha\beta} \\ \bar{N}^{ir}_{\alpha\beta} \end{Bmatrix} = \begin{bmatrix} A_{\alpha\beta\gamma\omega} & B^k_{\alpha\beta\gamma\omega} & E^s_{\alpha\beta\gamma\omega} & E^{su}_{\alpha\beta\gamma\omega} \\ B^j_{\alpha\beta\gamma\omega} & D^{jk}_{\alpha\beta\gamma\omega} & F^{sj}_{\alpha\beta\gamma\omega} & F^{suj}_{\alpha\beta\gamma\omega} \\ E^i_{\alpha\beta\gamma\omega} & F^{ik}_{\alpha\beta\gamma\omega} & E^{is}_{\alpha\beta\gamma\omega} & E^{isu}_{\alpha\beta\gamma\omega} \\ E^{ir}_{\alpha\beta\gamma\omega} & F^{irk}_{\alpha\beta\gamma\omega} & E^{irs}_{\alpha\beta\gamma\omega} & E^{irsu}_{\alpha\beta\gamma\omega} \end{bmatrix} \begin{Bmatrix} \epsilon_{\gamma\omega} \\ \epsilon^k_{\gamma\omega} \\ \bar{\epsilon}^s_{\gamma\omega} \\ \bar{\epsilon}^{su}_{\gamma\omega} \end{Bmatrix}
$$

$$
\begin{Bmatrix} Q_{\alpha 3} \\ Q^j_{\alpha 3} \\ \bar{Q}^i_{\alpha 3} \end{Bmatrix} = \begin{bmatrix} A_{\alpha 3\beta 3} & B^k_{\alpha 3\beta 3} & E^s_{\alpha 3\beta 3} \\ B^j_{\alpha 3\beta 3} & D^{jk}_{\alpha 3\beta 3} & F^{sj}_{\alpha 3\beta 3} \\ E^i_{\alpha 3\beta 3} & F^{ik}_{\alpha 3\beta 3} & E^{is}_{\alpha 3\beta 3} \end{bmatrix} \begin{Bmatrix} \gamma_{\beta 3} \\ \gamma^k_{\beta 3} \\ \bar{\gamma}^s_{\beta 3} \end{Bmatrix}
\tag{22}
$$

where $A_{\alpha\beta\gamma\omega}$, $B^j_{\alpha\beta\gamma\omega}$, etc. are the stiffnesses of the laminate. The explicit form of laminate stiffnesses is provided in Ref. 18.

E. Finite Element Model

The generalized displacements $(u_\alpha, u_3, u^j_\alpha, \bar{u}^i_\alpha, \bar{u}^i_3)$ are expressed over each element as a linear combination of the one-dimensional Lagrangian interpolation function ψ_l associated with node l and the nodal values $(u_\alpha)_l$, $(u_3)_l$, $(u^j_\alpha)_l$, $(\bar{u}^i_\alpha)_l$, and $(\bar{u}^i_3)_l$:

$$
\left(u_\alpha, u_3, u^j_\alpha, \bar{u}^i_\alpha, \bar{u}^i_3\right) = \sum_{i=1}^{n}\left[(u_\alpha)_l, (u_3)_l, \left(u^j_\alpha\right)_l, \left(\bar{u}^i_\alpha\right)_l, \left(\bar{u}^i_3\right)_l\right]\psi_l
\tag{23}
$$

where n is the number of nodes in a typical finite element. Substituting these expressions into the weak statement in Eq. (12), the finite element model of a typical element can be obtained as

$$[K(\Delta)]\{\boldsymbol{\Delta}\} = \{\boldsymbol{F}\} \tag{24}$$

where $[K(\Delta)]$ is the element stiffness matrix given by

$$[K(\Delta)] = [K(\Delta)]_L + [K(\Delta)]_{NL} \tag{25}$$

in which $[K]_L$ and $[K]_{NL}$ denote linear and nonlinear parts, respectively. $\{\boldsymbol{F}\}$ is the element force vector containing boundary and transverse force terms, and $\{\boldsymbol{\Delta}\}$ is the nodal displacement vector.

The expression for the element stiffness matrix $[K]$ and the force vector $\{\boldsymbol{F}\}$ are presented in Ref. 18. The solution of the nonlinear problem of Eq. (24) is obtained by using a Newton–Raphson iterative scheme.

F. Investigation of Contact Conditions

It is possible that the solution of Eq. (24) may indicate overlapping of the delaminated sublaminates during the postbuckling deformation even for a single delamination, depending on the direction and

magnitude of initial imperfection.[11,19] Thus, for accurate postbuckling analyses, preventing this physically inadmissible sublaminate overlapping phenomenon is necessary.

In the present study, a contact analysis is developed based on the assumption that the contact is frictionless ($\bar{u}_\alpha$ is not specified). The present approach allows for an accurate determination of the overlap regions and has the capability to correct this problem. Variational formulation of the present theory gives the boundary conditions associated with $\bar{u}_3^i$ (the opening displacement across the delamination), which can be interpreted as a contact condition of the ith delamination surfaces, and $\bar{Q}_3^i$ can be interpreted as the contact force at the ith delamination. At contact points, therefore, the delamination opening $\bar{u}_3^i$ must be zero and contact force $\bar{Q}_3^i$ must be nonzero.

The implementation of the contact algorithm is as follows.

1) Solve Eq. (24) for the displacements.

2) Identify the point of maximum overlap and specify essential boundary condition $\bar{u}_3^i = 0$ at that node.

3) Rerun the problem with the modified boundary condition.

4) Repeat procedures 2 and 3 until all overlaps disappear.

For the postbuckling analysis, initial imperfections are specified and the solution is calculated at the first load step using the Newton–Raphson method. The applied load N is then increased to $N + \Delta N$, and the process is repeated until the overlapping disappears. That is, the contact process is carried out at each Newton–Raphson iteration step. After the solution is obtained at a given load step, the applied load is increased, and the computational algorithm is repeated.

III. Numerical Results and Discussion

A. Single Delamination

The problem geometry is illustrated in Fig. 2. For convenience, the following nondimensional quantities are used:

$$\bar{t} = t/h, \qquad P = N/N_{\text{cr}}, \qquad \bar{a} = a/l \tag{26}$$

where N is the axial load applied to a composite and N_{cr} is the critical buckling load of the undelaminated composite. The material being used in this study is T300/5208 graphite/epoxy with typical properties of $E_{11} = 181$ GPa, $E_{22} = 10.3$ GPa, $G_{12} = G_{13} = 7.17$ GPa, and $\nu_{12} = \nu_{13} = 0.28$.

1. *Effects of Initial Imperfections and Contact Condition*

A specially orthotropic clamped composite laminate containing a single through-the-width delamination at its center with $\bar{t} = 0.2$ and $\bar{a} = 0.3$ is considered. The thickness-to-span ratio is assumed to be $h/l = 1/400$. The high-thickness-to-span ratio used in this example is intended to represent a thin laminate with a large delamination near its surface. For example, the combinations of the nondimensional parameters used in this example represent a 10-in.-long 5-ply unidirectional laminate, with ply thicknesses of 0.005 in., which has a 3-in. delamination under its first layer.

To satisfy the clamped boundary conditions, the initial imperfection is taken as

$$\begin{aligned} \xi &= \tfrac{1}{2} w_o h[1 - \cos(2\pi x_1/l)] \\ \bar{\xi}^i &= \tfrac{1}{2} \bar{w}_o^i h\left[1 - \cos\left(2\pi \bar{x}_1^i/a_i\right)\right] \end{aligned} \tag{27}$$

where, as shown in Fig. 2, h is the thickness and l the length of the plate, respectively. In Eq. (27), w_o is the fraction of initial deflection with respect to the plate thickness at the center and $\bar{w}_o^i$ is the fraction of initial opening of the ith delamination with respect to the plate thickness at the center. Bifurcation analysis predicts that the nondimensional buckling load for this problem is $P = 0.436$.

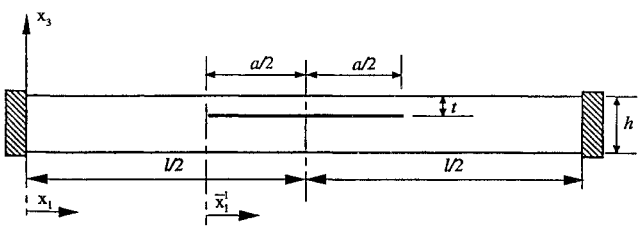

Fig. 2 Geometry of a clamped beam plate containing a through-the-width delamination.

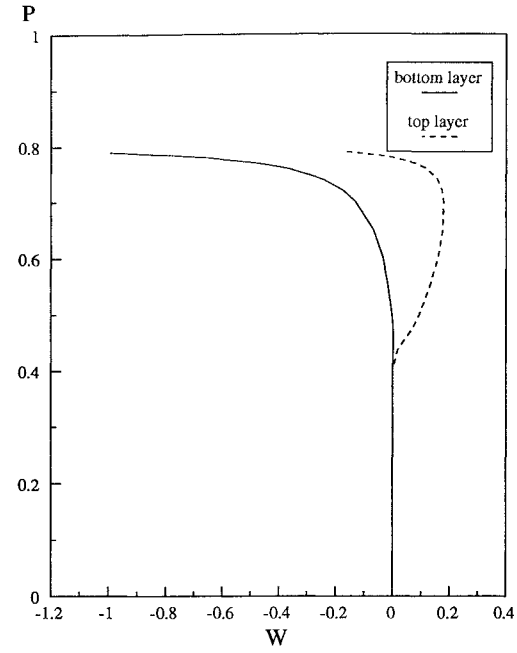

Fig. 3 Load-deflection curve of a delaminated composite with imperfection of $w_o = 0.001$.

The postbuckling solutions of this laminate for various initial imperfections are discussed in the following paragraphs. The out-of-plane deflection in these discussions is normalized as $W = u_3/h$ at the center of the beam plate. First, the initial imperfection is assumed to be the same shape as the buckling mode. In this case, the ratio of global imperfection w_o with respect to the local imperfection $\bar{w}_o^i$ is 0.008/1. For all the other cases, the initial delamination opening $\bar{w}_o^i$ is set to zero, thus only the global initial imperfection w_o is used.

The load-deflection curve with small magnitude of positive initial imperfection, $w_o = 0.001$, is shown in Fig. 3. As soon as the composite reaches the buckling load ($P = 0.436$), the top thin delaminated layer starts to buckle in the positive x_3 direction because the imperfection is positive, and the bottom thick layer gradually deflects in the negative x_3 direction. At $P = 0.7$, the deformation of the top layer is reversed, rendering the top layer substantially deflected downward. Finally, both layers lose load-carrying capacity at $P = 0.8$.

For larger magnitudes of positive imperfections (Fig. 4), the response is significantly different. For example, for $w_o = 0.1$ the delamination buckling load is not distinguishable, and the composite starts to deflect upward with a delamination opening as soon as the load is applied. Furthermore, above the load level of $P = 0.8$, the two layers overlap, suggesting the necessity of contact condition.

To investigate the effect of contact more rigorously, relatively small and large negative initial imperfections, $w_o = -0.001$ and -0.1, are considered. The load-deflection curves for $w_o = -0.001$ are shown in Fig. 5 for the analyses with and without contact condition. For the case without contact condition, since the top layer has larger negative displacement than the bottom layer, it penetrates the bottom part above the buckling load level. Sheinman and Souffer[11] obtained this physically inadmissible postbuckling deformation for a delaminated beam and suggested that local buckling may not occur for this deformation process. When the contact condition is imposed on the problem, however, the postbuckling response is surprisingly different from the one where overlapping is permitted. Until the buckling load, both parts press against one another, with negligibly small contact force. At the buckling load ($P = 0.436$), the contact force is suddenly increased due to the top layer, which tries to buckle down (overlap). Since the bending stiffness of the bottom layer is much higher than that of the top part, the bottom layer does not deflect, and the top layer snaps through and buckles up. Further studies showed that for this small negative magnitude of imperfection the

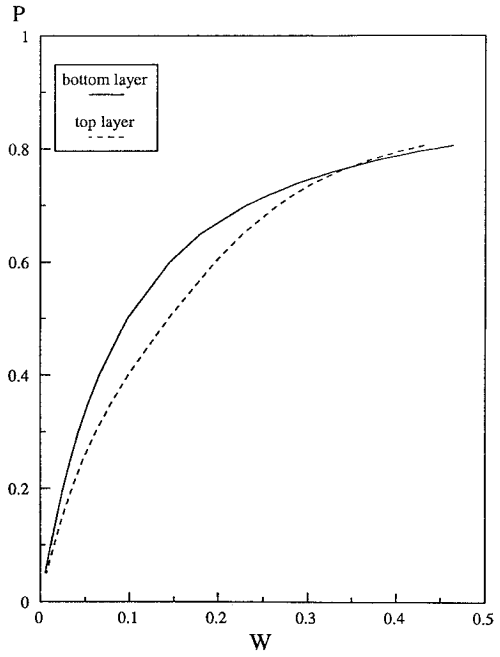

Fig. 4 Load-deflection curve of a delaminated composite with imperfection of $w_o = 0.1$.

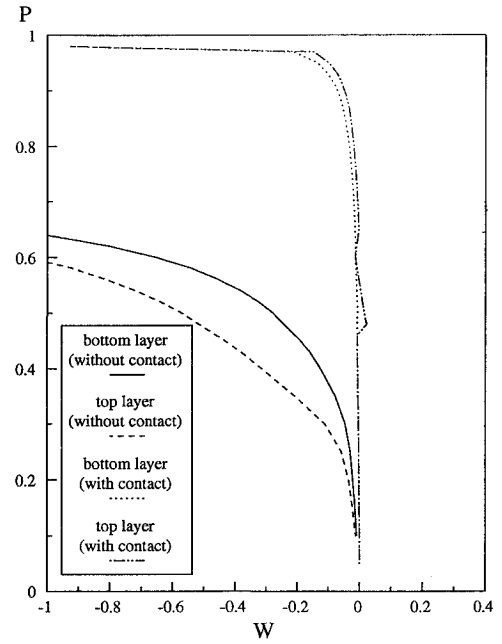

Fig. 6 Load-deflection curve of a delaminated composite with imperfection of $w_o = -0.1$.

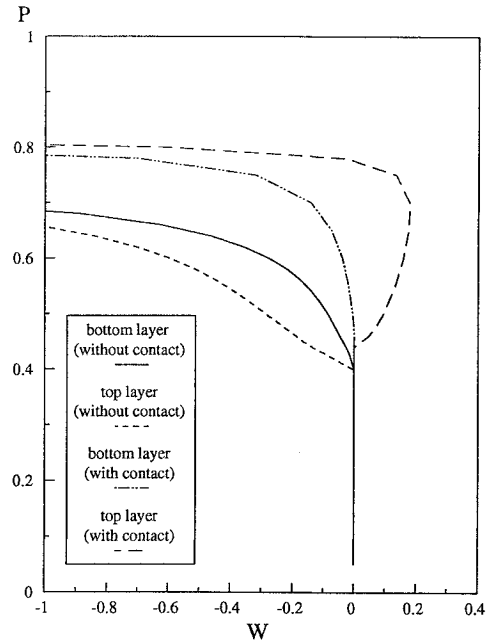

Fig. 5 Load-deflection curve of a delaminated composite with imperfection of $w_o = -0.001$.

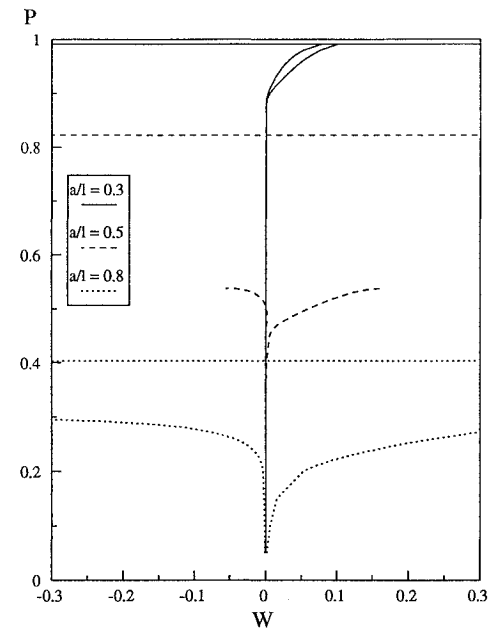

Fig. 7 Load-deflection curve of $[0/90/90//0]_T$ laminate.

global equilibrium path is the same as the case for $w_o = 0.001$, and they are almost identical to the result obtained in Fig. 3 for a beam with small imperfections of positive magnitude.

For the larger negative initial imperfection, $w_o = -0.1$, shown in Fig. 6, the load deflection curve again shows a physically unacceptable deformed mode when the contact condition is not applied. On the other hand, the curve with contact condition shows a significantly different deformation pattern. This time, the delamination effect is negligible. The plate behaves as if there is no delamination in it. In fact, the delamination opens slightly at the buckling load, but the opening is so small that it does not affect the global behavior of the structure. Accordingly, the failure may occur at the load level of the undelaminated plate case ($P = 1$).

2. Effect of Stacking Sequence

Even an initially symmetric laminate can be locally unsymmetric when it contains a delamination and may, thus, exhibit bending-extension coupling. In the following example, this type of bending-extension coupling effect is studied for $[0/90/90//0]_T$ and $[90/0/0//90]_T$ simply supported cross-ply laminates. Here, the double solidus denotes an interface where a delamination lies. The thickness-to-span ratio is assumed to be 1/10, and three delamination lengths $\bar{a} = 0.3, 0.5$, and 0.8 are considered. Note that initial imperfection is not required to initiate the postbuckling deformation for simply supported boundary conditions, because a delamination itself has the effect of an imperfection. As a result, no initial imperfection is used in this analysis.

The normalized out-of plane deflection for these cases are shown in Figs. 7 and 8. The horizontal lines in Figs. 7 and 8 indicate buckling loads calculated from linear bifurcation analysis for each of the delamination lengths. Load-deflection curves for the $[0/90/90//0]_T$ laminate are shown in Fig. 7. For all delamination lengths, the bottom sublaminate tends to deflect downward immediately due to bending-extension coupling. But for $\bar{a} = 0.3$, the debonded region is relatively small compared with the entire length of the composite;

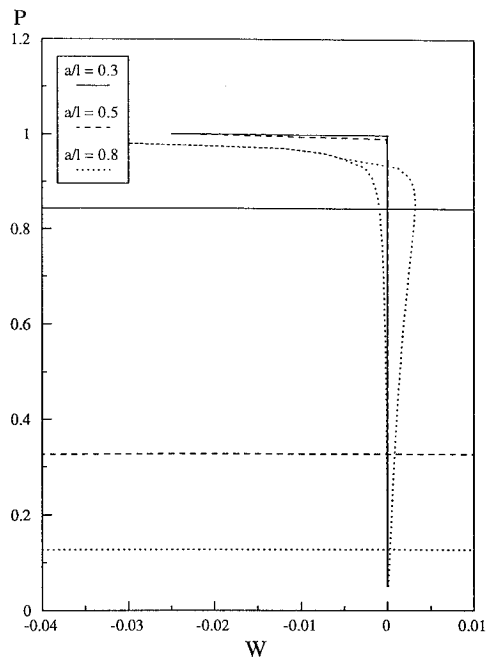

Fig. 8 Load-deflection curve of $[90/0/0//90]_T$ laminate.

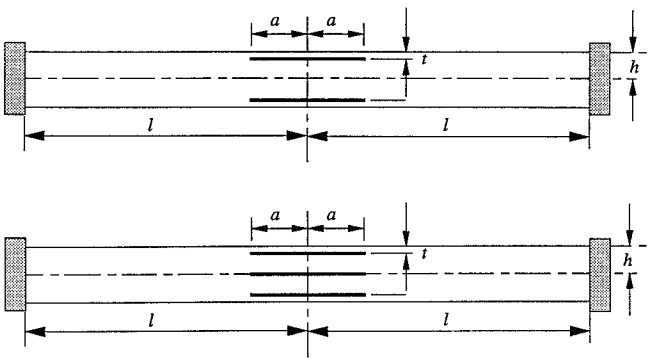

Fig. 9 Two and three symmetrically located delaminations.

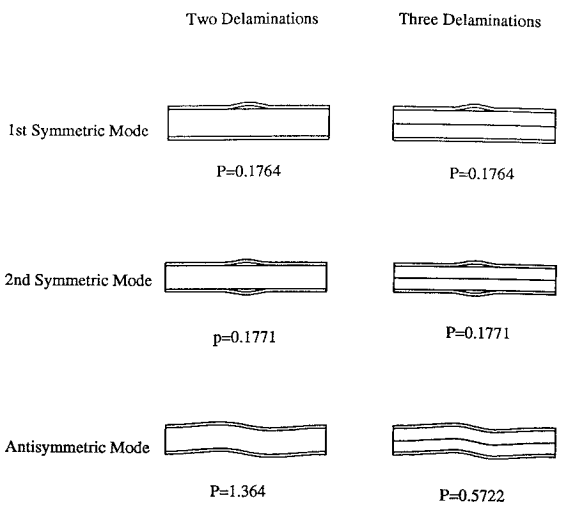

Fig. 10 Buckling loads and mode shapes for two and three delaminations.

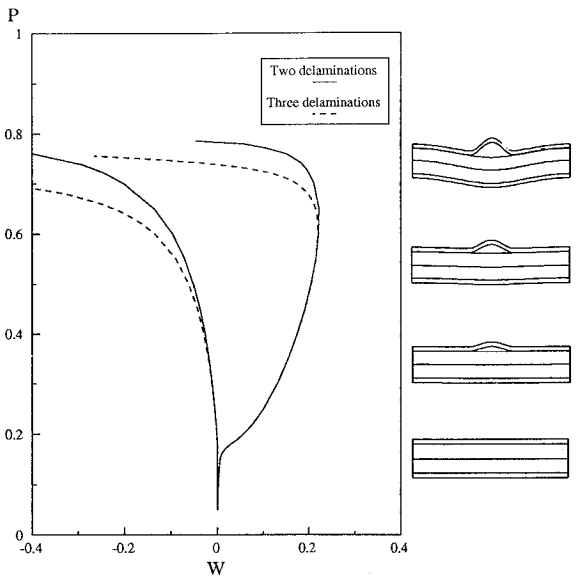

Fig. 11 Load-deflection curve for a composite containing two and three delaminations with imperfection of the first symmetric buckling mode.

thus, the coupling effect is negligible. For $\bar{a} = 0.5$ and 0.8, on the other hand, the laminate loses its load-carrying capacity well below the predicted buckling load, and the delamination opens rapidly due to the coupling.

In contrast to the $[0/90/90//0]_T$ laminate, the bottom sublaminate of the $[90/0/0//90]_T$ stacking sequence tends to deflect upward due to the bending-extension coupling. At the same time, the compliant top layer cannot carry the load, resulting in the eccentricity which causes the bottom part to buckle downward. These two effects balance each other, and the structure remains straight with a very small delamination opening until the buckling load level of the undelaminated plate is reached, as shown in Fig. 8, regardless of the delamination length. It is shown that the predicted buckling load significantly underestimates the global buckling of the structure. That is, contrary to conclusions of other investigators,[10,11] in this case the bending-extension coupling is shown to have a stabilization effect on the buckling of a delaminated composite. The significant disagreement of buckling loads between the eigenvalue and postbuckling analyses is a result of the prebuckling effects that are neglected in the eigenvalue analysis.

B. Multiple Delaminations

An example by Lee et al.[15] is reconsidered here see (Fig. 9). This example demonstrates the effects of varying the through-the-thickness position and the number of delaminations on the postbuckling behavior. Two delaminations symmetrically located with respect to midplane and three delaminations with an additional one at the midplane are investigated. All delaminations are assumed to have the same length. The material properties of random short-fiber SMC-R50 composite considered in this study are as follows[20]: $E_{11} = 10.9$ GPa, $E_{22} = 7.58$ GPa, $G_{12} = G_{13} = 2.48$ GPa, $\nu_{12} = 0.31$, and $\nu_{13} = 0.22$.

To investigate the deformation process of the compressed composite with multiple delaminations, postbuckling analyses are presented for $\bar{a} = 0.3$ and $\bar{t} = 0.25$. The first two or three lowest symmetric buckling mode shapes and an antisymmetric mode are shown in Fig. 10. It can be seen that the several lowest buckling loads are very close to one another. For this reason, the postbuckling solution is obtained for imperfections of these mode shapes.

For all of the results presented, the magnitudes of the initial imperfections (w_o and $\bar{w}_o^i$) are determined in the following way. First, calculate the buckling mode and identify the ratio of the deflections of each sublaminate at the center of the composite. Second, set the maximum deflection from the buckling mode to 1×10^{-3} as an imperfection (either w_o or $\bar{w}_o^i$ depending on the mode shape), and set the others according to the ratio in the buckling mode.

Load-deflection curves are shown in Figs. 11 and 12 for $\bar{t} = 0.25$ with initial imperfections of the first and the second buckling mode shapes. For the first mode imperfection (Fig. 11), the lower delamination always remains closed, and the composite acts as if it contains only the upper delamination. For the second mode imperfection (Fig. 12), both delaminations start to open at the buckling load. As the load level approaches $P = 0.75$, the beam buckles abruptly.

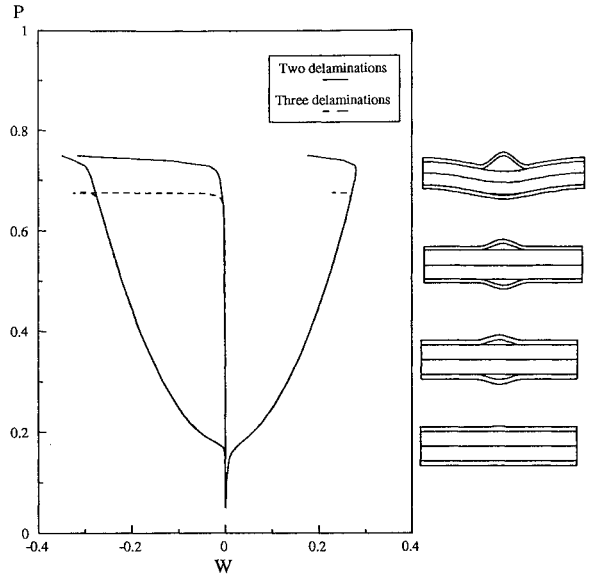

Fig. 12 Load-deflection curve for a composite containing two and three delaminations with imperfection of the second symmetric buckling mode.

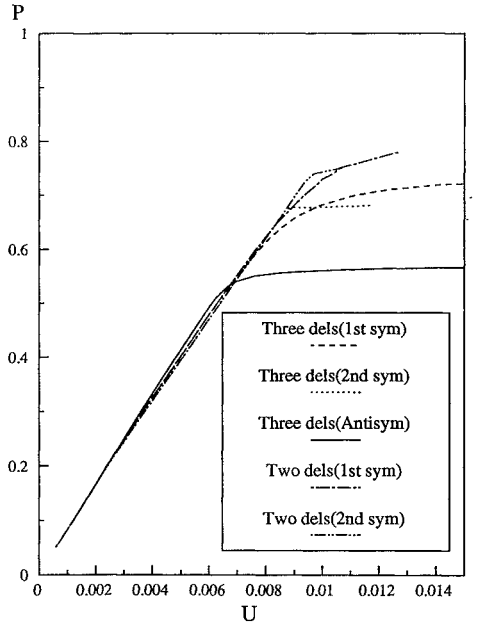

Fig. 13 Load-end shortening curve for a composite containing two and three delaminations with various initial imperfections.

For three delaminations, the load-deflection curves show the same trends as that of the two delamination cases for both the first- and the second-mode imperfections. The bifurcation points for both cases are the same as the first and the second buckling mode shapes, respectively. However, the ultimate load-carrying capacity for the three delamination cases are slightly below the two delamination cases.

The load-end shortening relation is illustrated in Fig. 13 for two and three delaminations with $\bar{t} = 0.25$. For three delaminations, the load-end shortening curve for the antisymmetric case coincides with the symmetric cases until the load reaches the first buckling load ($P = 0.1764$). Above this load level, the slopes of the curves for symmetric modes change slightly, whereas the antisymmetric case continues as an extension of the prebuckling path. At a buckling load of the antisymmetric mode ($P = 0.5722$), the composite with the antisymmetric mode can no longer sustain the load. Usually, it is known that a sudden buckling mode change may occur when two end-shortening curves cross each other.[21] It should be noted here that the curves with symmetric and antisymmetric modes do not necessarily represent the postbuckling deformed mode change phenomenon. As a consequence, although the buckling load for the antisymmetric mode shape is far beyond that of the symmetric mode shape, the final load-carrying capacity of the antisymmetrically buckled composite is substantially lower than that of the symmetric modes. This implies that as soon as a delaminated composite buckles in an antisymmetric mode, it cannot carry the load and, thus, does not exhibit postbuckling deformation.

IV. Concluding Remarks

A one-dimensional, layerwise finite element model is developed to study the postbuckling behavior of composite plates with through-the-width delaminations. The model is capable of predicting accurate postbuckling response for both single and multiple delaminations. The effects of composite geometry and locations, sizes, and number of delaminations on postbuckling behavior of composites are studied. The effects of stacking sequence, contact behavior of delaminated surfaces, and initial imperfections of composites are also considered.

Based on the theoretical developments and numerical results, the following concluding remarks are made.

1) The postbuckling response of a delaminated composite is very sensitive to the amplitude and direction of initial imperfection, especially for near-the-surface delaminations. This is because there are many equilibrium paths, and the composite can take any path depending on the initial imperfections. For a relatively large magnitude of imperfection in the direction of the thicker sublaminate, delamination buckling does not occur, showing that the presence of this imperfection has a beneficial contribution on the postbuckling response of a delaminated composite.

2) The effect of anisotropy on the buckling and postbuckling response of delaminated composites is significant. The linear bifurcation analysis for highly anisotropic sublaminates may lead to erroneous results, and accordingly postbuckling analysis is necessary. For compliant inner and stiff outer layers of $[0/90/90//0]_T$ laminate the bending-extension coupling significantly reduced the buckling load and increased the postbuckling deformation. For stiff inner and compliant outer layers of $[90/0/0//90]_T$ laminate, however, the coupling is shown to have a stabilization effect for delamination buckling and postbuckling deformation, contradicting the conclusions of some of the previous researchers. This is because the contact effects of delaminated surfaces were neglected in those previous works.

3) For some configurations of multiple delaminations, although the first buckling load for the antisymmetric mode is much greater than for the symmetric mode, the ultimate load-carrying capacity is significantly lower than the symmetric case due to the unstable nature of the antisymmetric mode. In this case, a sudden mode change in postbuckling deformation is expected.

References

[1]Chai, H., Babcock, C. D., and Knauss, W. B., "One-Dimensional Modeling of Failure in Laminated Plates by Delamination Buckling," *International Journal of Solids and Structures*, Vol. 17, No. 11, 1981, pp. 1069–1083.

[2]Simitses, G. J., Sallam, S., and Yin, W. L., "Effect of Delamination of Axially Loaded Homogeneous Laminated Plates," *AIAA Journal*, Vol. 23, No. 9, 1985, pp. 1437–1444.

[3]Sallam, S., and Simitses, G. J., "Delamination Buckling and Growth of Flat Cross-Ply Laminates," *Composite Structures*, Vol. 4, No. 4, 1985, pp. 361–381.

[4]Yin, W. L., Sallam, S., and Simitses, G. J., "Ultimate Axial Load Capacity of a Delaminated Beam-Plate," *AIAA Journal*, Vol. 24, No. 1, 1986, pp. 123–128.

[5]Bolotin, V. V., Zebelyan, Z. K., and Kurzin, A. A., "Stability of Compressed Components with Delamination-Type Flaws," *Problemy Prochnosti*, No. 7, July 1980, pp. 3–8.

[6]Kardomateas, G. A., and Schmueser, D. W., "Buckling and Postbuckling of Delaminated Composites under Compressive Loads Including Shear Effects," *AIAA Journal*, Vol. 26, No. 3, 1988, pp. 337–343.

[7]Kardomateas, G. A., "Large Deformation Effects in the Postbuckling Behavior of Composite with Thin Delaminations," *AIAA Journal*, Vol. 27, No. 5, 1988, pp. 624–631.

[8]Chen, H. P., "Shear Deformation Theory for Compressive Delamination Buckling and Growth," *AIAA Journal*, Vol. 29, No. 5, 1991, pp. 813–819.

[9]Sheinman, I., Bass, M., and Ishai, O., "Effect of Delamination on Stability of Laminated Composite Strip," *Composite Structures*, Vol. 11, No. 3, 1989, pp. 227–242.

[10]Yin, W. L., "The Effects of Laminated Structures on Delamination Buckling and Growth," *Journal of Composite Materials*, Vol. 22, June 1988, pp. 502–517.

[11]Sheinman, I., and Souffer, M., "Postbuckling Analysis of Composite Delaminated Beams," *International Journal of Solids and Structures*, Vol. 27, No. 5, 1991, pp. 639–646.

[12]Suemasu, H., "Analytical Study of Shear Buckling and Postbuckling of Composite Plates with a Delamination," *Japan Society of Mechanical Engineers International Journal*, Ser. 1, Vol. 34, No. 2, 1991, pp. 135–142.

[13]Breivik, N. L., Gürdal, Z., and Griffin, O. H., "Compression of Thick Laminated Composite Beams with Initial Impact-Like Damage," *Journal of Reinforced Plastics and Composites*, Vol. 12, July 1993, pp. 813–824.

[14]Kutlu, Z., and Chang, F. K., "Modeling Compression Failure of Laminated Composites Containing Multiple Through-the-Width Delaminations," *Journal of Composite Materials*, Vol. 26, No. 3, 1992, pp. 350–387.

[15]Lee, J., Gürdal, Z., and Griffin, O. H., "Layer-Wise Approach for the Bifurcation Problem in Laminated Composites with Delaminations," *AIAA Journal*, Vol. 31, No. 2, 1993, pp. 331–338.

[16]Reddy, J. N., "A Generalization of Two Dimensional Theories of Laminated Composite Plates," *Communications in Applied Numerical Methods*, Vol. 3, No. 3, 1987, pp. 173–180.

[17]Chia, C. Y., *Nonlinear Analysis of Plates*, McGraw–Hill, New York, 1980, pp. 1–21.

[18]Lee, J., Griffin, O. H., and Gürdal, Z., "Vibration, Buckling and Postbuckling of Laminated Composites with Delaminations," Center for Composite Materials and Structures, CCMS Rept. 92-13, Virginia Polytechnic Inst. and State Univ., Blacksburg, VA, June 1992.

[19]Whitcomb, J. D., "Finite Element Analysis of Instability Related Delamination Growth,"*Journal of Composite Materials*, Vol. 15, Sept. 1981, pp. 403–426.

[20]Wang, S. S., Zahlan, N. M., and Suemasu, H., "Compressive Stability of Delaminated Random Short-Fiber Composites, Part II—Experimental and Analytical Results," *Journal of Composite Materials*, Vol. 19, No. 4, 1985, pp. 317–333.

[21]Stein, M., "Loads and Deformation of Buckled Rectangular Plates," NASA TR R-40, 1959.